Use of the Filter Diagonalization Method in the Study of Space Charge Related Frequency Modulation in Fourier Transform Ion Cyclotron Resonance Mass Spectrometry

ARTICLE *in* JOURNAL OF THE AMERICAN SOCIETY FOR MASS SPECTROMETRY · JULY 2006

Impact Factor: 2.95 · DOI: 10.1016/j.jasms.2006.02.018 · Source: PubMed

2 AUTHORS:

Konstantin Aizikov
Thermo Fisher Scientific
11 PUBLICATIONS **179** CITATIONS
SEE PROFILE

Peter O'Connor
The University of Warwick
101 PUBLICATIONS **2,413** CITATIONS
SEE PROFILE

Use of the Filter Diagonalization Method in the Study of Space Charge Related Frequency Modulation in Fourier Transform Ion Cyclotron Resonance Mass Spectrometry

Konstantin Aizikov*† and Peter B. O'Connor*

Mass Spectrometry Resource, Department of Biochemistry, Boston University School of Medicine, Boston, Massachusetts, USA

The filter diagonalization method (FDM) is a recently developed computational technique capable of extracting resonance frequencies and amplitudes from very short transient signals. Although it requires stable resonance frequencies and is slower than the fast Fourier transform (FFT), FDM has a resolution and accuracy that is unmatched by the FFT or any other comparable techniques. This unique feature of FDM makes it an ideal tool for tracing space charge induced frequency modulations in Fourier transform ion cyclotron resonance (FT-ICR) cells, which are shown to reach ±400 ppm even for such simple spectra as Substance P. (J Am Soc Mass Spectrom 2006, 17, 836-843) © 2006 American Society for Mass Spectrometry

With the increasing number of completed and nearly completed genomes, research interest is shifting to proteomics [1], which is the study of the structure and function of the translated proteins. Due to its high sensitivity, accuracy, and reproducibility, mass spectrometry is one of the primary technologies used in this field. One of the most important factors in identifying and sequencing proteins as well as identifying and localizing posttranslational modifications in proteins is the accuracy of the experimentally determined masses [2]. Fourier transform mass spectrometry (FTMS) [3–5] produces the best mass accuracy and resolving power currently available.

Current FTMS instruments are capable of routinely producing measurements with ~1 ppm accuracy internally calibrated [6–8] and ~5 ppm externally calibrated [9, 10]. Recent studies in proteomics show that determination of amino acid composition of tryptic peptides requires at least 0.1 ppm mass accuracy [11, 12]. One of the major fundamental factors determining FTMS mass accuracy limits is the "space-charge" effect, which arises from columbic interactions among ions within the FT-ICR cell, causing frequency shifts in time with periodicities equal to the beat frequencies of different ion packets (note, Wineland and Dehmelt [13] demonstrated that ions of the same *m/z* do not experience the same space charge induced frequency modulations that are observed between ions of different *m/z*). Due to the very fast nature of the "space-charge" phenomena, techniques for its analysis must operate on short transient signals. The fast Fourier transform (FFT) [14], however, is limited to a resolution of $\Delta\omega = 2\pi N\tau$, where N is the number of data points and τ is the sampling time, and cannot generally provide detailed information on frequency shifts within a transient.

Other FT based signal processing methods such as wavelet and chirplet [15] transforms as well as the shifted-basis technique [16], although having lower uncertainty, suffer from the same shortcoming of the resolving power being directly proportional to the length of the transient. On the other hand, high-resolution techniques such as linear prediction [17, 18] or Prony method based techniques [19, 20] are very computationally expensive.

The filter diagonalization method (FDM) [21–27] is a recently developed signal-processing algorithm based on a linear algebra mathematical formalism, which finds the exact solution of the harmonic inversion problem [27] and, theoretically, can achieve infinite resolution if the resonant frequencies are stable. FDM has been shown to provide superb accuracy on short transient signals and, compared to other high-resolution computational techniques, is very quick (e.g., FDM's time complexity scales quasi-linearly with the number of data points, which puts it in the same order as the FFT). These two factors make it an ideal tool for frequency shift chasing experiments as shown here. These results could be used for reference deconvolution [28, 29] to improve mass accuracy.

Theory

Although detailed description is available in the literature [21, 23–25, 27], a brief description of FDM's main features, structure, and functionality compiled from the

Published online April 17, 2006

Address reprint requests to Dr. P. B. O'Connor, Mass Spectrometry Resource, Department of Biochemistry, Boston University School of Medicine, Boston, MA 02118, USA. E-mail: poconnor@bu.edu

* Also at the Cardiovascular Proteomics Center, Boston University School of Medicine, Boston, MA.

† Also with the Bioinformatics Program, Boston University, Boston, MA.

1044-0305/06/$32.00
doi:10.1016/j.jasms.2006.02.018

Received August 31, 2005
Revised February 17, 2006
Accepted February 25, 2006

above references is provided since it is new in the field of FTMS. The main objective of FDM is to interpolate complex amplitudes d_k and complex frequencies ω_k from a time signal $C(t_n)$

$$C(t_n) = c_n \equiv \sum_{k=1}^{K} d_k e^{-in\tau\omega_k}, \quad (1)$$

which is defined on an equidistant time grid $t_n = n\tau$, $n = 0,1,\ldots,N-1$ with complex frequencies $\omega_k = 2\pi f_k - i\gamma_k$ (including damping γ_k), where N is the number of data points, τ is the time step, and f_k is the frequency in Hz. Even though the fitting problem of eq 1 is highly nonlinear, the solution can be obtained by pure linear algebra if one assumes Lorentzian line shape and uniform sampling rate.

The unique feature of FDM is the association of c_n with a time correlation function of a hypothetical quantum system described by a complex symmetric Hamiltonian operator $\hat{\Omega}$ with complex eigenvalues ω_k and the initial state Φ_0

$$c_n = \left(\Phi_0 | e^{-in\tau\hat{\Omega}} \Phi_0\right), \quad (2)$$

which redefines the problem of fitting the observed time signal c_n to eq 1 as one of diagonalizing $\hat{\Omega}$ or, equivalently, its evolution operator $\hat{U}$ over a single step, where $\hat{U} = e^{-i\tau\hat{\Omega}}$. Furthermore if Y_k is a set of orthonormal eigenvectors, which diagonalizes $\hat{U}$, then

$$\hat{U} = e^{-i\tau\hat{\Omega}} = \sum_k e^{-i\tau\omega_k} |Y_k)(Y_k| \quad (3)$$

and from eqs 1, 2, and 3 corresponding abundance values, d_k, can be calculated as

$$d_k = (\Phi_0 | Y_k)(Y_k | \Phi_0) = (Y_k | \Phi_0)^2 \quad (4)$$

Although neither $\hat{\Omega}$ nor $\hat{U}$ are explicitly available, their matrix elements in an appropriately chosen basis can be reconstructed from the observed time signal. For instance, $\hat{U}$ can be reconstructed using Krylov type finite-time Fourier [26] basis described by

$$\psi_j - \psi(z_j) = \sum_{n=0}^{M} \left(\hat{U} | z_j\right)^n \Phi_0, \quad (5)$$

where $z_j = e^{-i\phi_j}$, $\phi_j = \omega_j\tau$, $\phi_{\min}/\tau < \omega_k < \phi_{\max}/\tau$, $j = 1, 2, \ldots, K_{win}$, and the matrix elements (note, the basis is not orthonormal) can be obtained from

$$U^{(p)}(\phi_j, \phi_{j'}) = U^{(p)}[j, j'] = (\psi_j | \hat{U}^p \psi_j = \sum_{n=0}^{M}\sum_{n'=0}^{M} (z_{j'}/z_j)^n c_{n+n'+p} z_{j'}^{-(n+n')}, \quad (6)$$

where $p = 0,1,2\ldots$, and M is the one half of the transient length. Now, the fitting problem of eq 1 is recast into generalized eigenvalue problem

$$U^{(1)} B_k = u_k U^{(0)} B_k, \quad (7)$$

where $u_k = e^{-i\tau\omega_k}$ are eigenvalues and B_k are eigenvectors of the system, note that B_k are normalized with respect to $U^{(0)}$, and the intensities d_k can be recovered [22, 26] as

$$\sqrt{d_k} = \sum_{j=1}^{k_{win}} B_{jk} \sum_{n=0}^{M} c_n \quad (8)$$

By using a rectangular window Fourier basis eq 6, and moving into the frequency domain where interaction between adjacent points is small and the matrices are diagonally dominant with the richest informational content along the main diagonal [22] the computational effort for solving the generalized eigenvalue problem eq 7 becomes much smaller. More importantly, the size of the matrices, $K_{win,}$ can be relatively small, in practice ranging from 3 to 100 [22]. These two factors let us achieve quasi-linear computational complexity, which is comparable to that of FFT. However, construction of the $\hat{U}$ matrices imposes a large constant prefactor so that while FDM scales well, it is slower than the FFT.

One of the major advantages of FDM over FFT is its resolution. The Fast Fourier Transform is limited in peak width to $\Delta\omega = 2\pi/N\tau$. In theory FDM can have infinite resolution. In practice, infinite resolution is achievable only if the local average density of peaks $P(\omega)$ satisfies

$$\rho(\omega) \equiv 2\pi/\delta\omega \leq N\tau/2, \quad (9)$$

where $\delta\omega$ is the spacing between the adjacent peaks [23].

While FDM has a resolution advantage which is reported in this manuscript, it also has some disadvantages compared to FFT. Specifically, the local nature of the basis can generate spurious values or "false" solutions to eq 7. These spurious values, while annoying, can be purged. There are a number of ways to get rid of them [21] but the most simple and efficient one is solving eq 7 for overlapping K_{win} and dropping out those solutions which appear only once [21]. Furthermore, because it is not an approximation technique and solves eq 1 exactly, FDM experiences substantial difficulties in cases when the frequencies are not stable, for example under "space-charge" conditions.

Methods

In this study an in-house C++ implementation of the FFT square window FDM was used, which is integrated into the Boston University Data Analysis (BUDA) system [30] and is available as open source software. The constructions of the matrices described by eqs 11 and 12 were implemented following the method described by Hu et al. [22]. To make the calculations faster, the FFTW implementation of the FFT [31] was used in place of the discrete FT as described in the above reference. Use of the FFT limited the granularity of the $\Delta\omega$, or to be more precise the spacing between adjacent frequencies φ_j in eq 6, to $2\pi/N\tau$ and

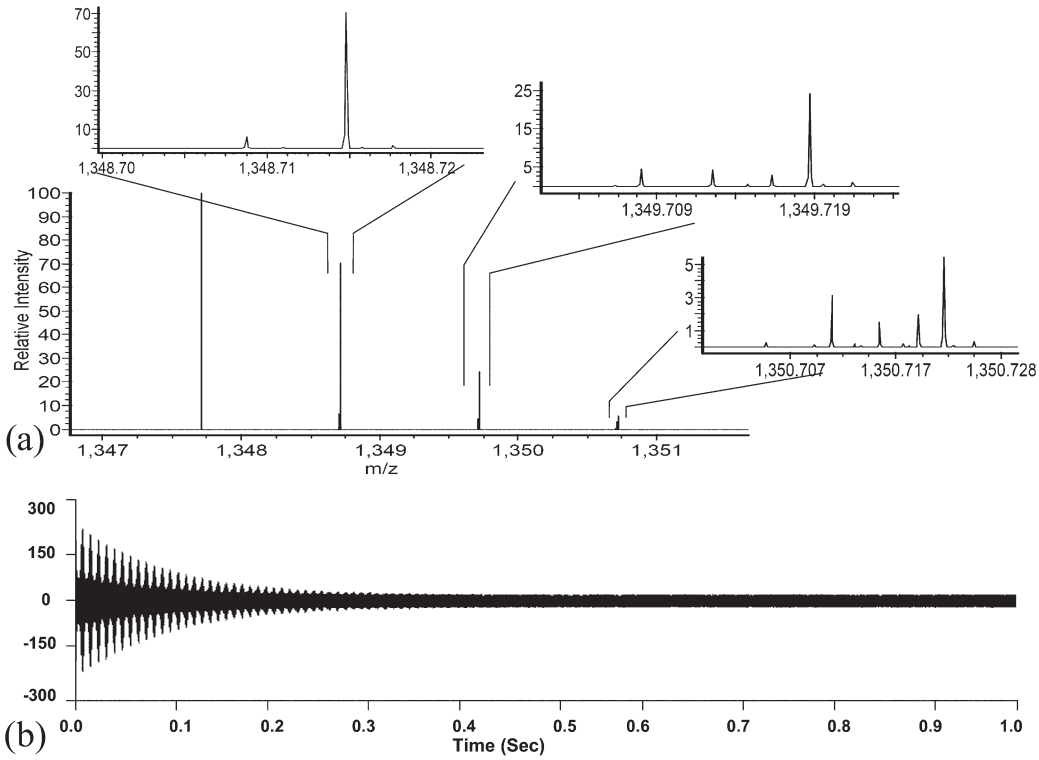

Figure 1. (**a**) Theoretical Mass spectrum of Substance P using isotopic abundances calculated by IsoPro 3.0 (*m/z* versus Relative Intensity) and (**b**) the corresponding transient signal of 1 s (1M data points) duration sampled at 1MHz rate with the dumping constant of 10. The signal was generated using stable frequencies.

consequently increased the minimal length of the transient signals necessary to provide the same accuracy (for the spectra used, the transient length of 1 millisecond or 1K data points generally satisfied the criteria for selected peaks). Modified CLAPAC code [32] was used for solving the generalized eigenvalue problem.

For testing the FDM implementation, theoretical spectra were generated in-house with 1 mega-point lengths and 1 MHz sampling rate based on isotopic abundances calculated using IsoPro 3.0 [33, 34]. The conversion from *m/z* to frequency domain was done according to the calibration equation $f = \frac{z}{m}A - B$ where $A = 107079830.92$ and $B = -0.69$, which differ slightly from the values used in the calibration of the experimental spectra, this caused a slight difference in frequency domain between the two. Real spectra of Substance P were acquired on a homebuilt ESI FTMS instrument [35–37] (1 mega-point length with 1 MHz acquisition rate). Frequency chasing experiments were performed on transient domains ranging from 1000 to 20,000 data points starting with the 0 offset and shifting depending on the experiment from 1 to 200 data points into transient. K_{win} ranged from 4 to 11 points.

Results and Discussion

To test the fundamental capabilities of FDM, theoretical spectra were generated where the exact signal composition was defined a priori with an absence of frequency shift modulation. A theoretical transient signal (Figure 1) of length 1 s (1 M data points) with sampling rate of 1 MHz and damping of 10 s^{-1} was generated using frequencies and abundances from the table in the Supplementary Material section (which can be found in the electronic version of this article) calculated from the known elemental composition of Substance P using IsoPro 3.0 [33, 34]. In particular, the fine structures of the A + 1, A + 2, and A + 3 isotopes were included. (The A ion at 1347.712, being the monoisotopic peak, has no fine structure). Performance studies of the two methods were conducted on the first 1, 0.5, 0.25, 0.1, 0.01, and 0.001 s of the transient (Figure 2). Note that while the FFT generates a spectrum and then peak centroids must be calculated from it by nonlinear least-squares fitting, FDM first generates a line list by solving eqs 7 and 8, and Figure 2 (right) is generated subsequently by applying a sum of Lorentzian line shapes to the data in Table 1. Figure 2 clearly shows that the FFT fails to resolve the fine structure of the spectrum (producing only the major peaks) even at 1M points (1.0 s.) with 80,000 resolving power (Figure 1a) and fails to resolve even the main isotopic peaks when the first 0.01 s (Figure 2e) of the signal is used. In contrast, FDM produces all the peaks from the Supplementary Material table at 0.25 s and some peak merging takes place as the signal is shortened beyond the limit imposed by eq 13 for these peaks. FDM, however, still produces a bona fide isotopic distribution with reasonably good abun-

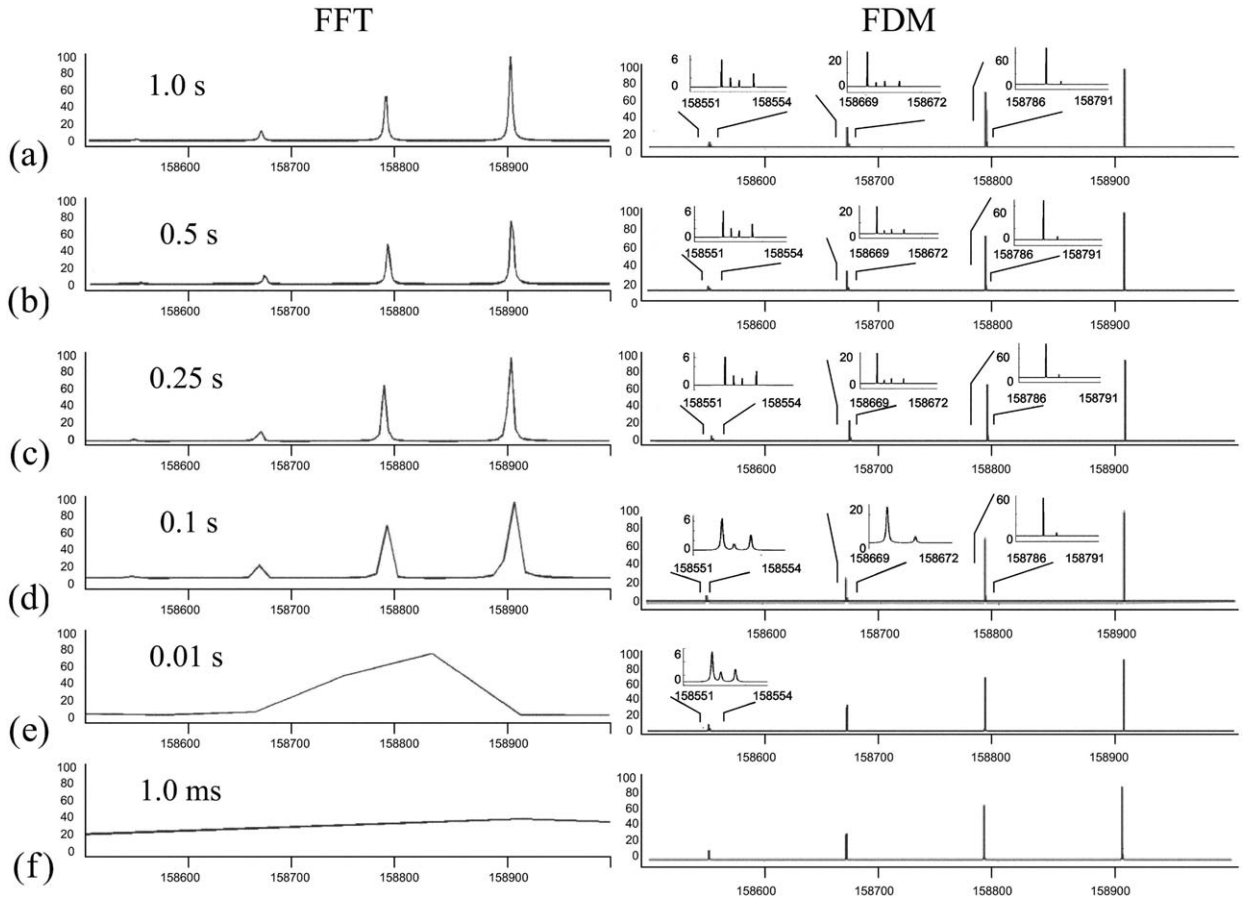

Figure 2. Frequency spectrum recovered from the first (**a**) 1M, (**b**) 0.5 M, (**c**) 0.25M, (**d**) 0.1M, (**e**) 0.01M, and (**f**) 1000 data points of the transient signal in Figure 1b using the FFT (left) and using the FDM (right). The FDM "spectrum" is constructed from a Lorentzian fit to the peak list from Table 1.

dance ratios even when the transient length is only 1 ms (Table 1e). This aspect of FDM algorithm could be particularly useful for mass spectrometry of short-lived radionuclides [38].

In general, the peak merging is a result of the violation of inequality eq 13. These merged peaks can be thought of as poorly resolved peaks [23]. The merging is accompanied by increase in error (Table 1), or the difference between the peaks recovered by the overlapping K_{win}. This error serves as an uncertainty measure and has been used to filter out the spurious peaks [21]. Note that, even with a 1 ms transient, the monoisotopic peak at 158,906.79 Hz is resolved almost exactly with an error of $\sim 7*10^{-4}$ ppm. In general, as long as condition eq 13 holds the FDM is capable of achieving "infinite" resolution [20], with errors only due to noise and inherent computational round off errors.

Although FDM performance in terms of accuracy on signals with no frequency modulation is by far superior to that of FFT, FDM, whose main assumption is that the resonant states are stable, does not perform that well when frequency shifts are substantial. Thus, it generally fails to provide better mass accuracy when used in place of FFT on real FTMS signals. However, the ability to lock in on frequencies in extremely short transients (as seen in the previous example, Figure 2) implies that FDM is a good tool for studying frequency shifts during FTMS experiments. To test the performance of FDM in following shifts through a transient, a theoretical signal of 0.5 s length was generated, where 140,080.1276 Hz frequency was modulated through 0.0005 Hz (3.6 ppb) with a frequency of 10 Hz (Figure 3), and sampled at 1 MHz with signal to noise ratio of 2 in the time domain. The frequency chasing experiment was performed with 0.5 millisecond (500 data points) transient domains stepping 200 data points into the raw data. While the signal to noise ratio of 2 in the theoretical signal, input to the FDM algorithm, clearly resulted in some noise in the output, the FDM was able to create an output signal that reproduced the frequency versus time plot from Figure 3a with sub ppb accuracy. Note, that FDM also generated several spurious glitches, which were discussed above.

The same frequency chasing experiments were conducted on a real Substance P spectrum (Figure 4) chasing the three major isotopic peaks using 20 millisecond transient domains (20,000 data points) stepping 200 data points into the transient for each FDM calculation through the first 0.5 S of the transient. This calculation produced the frequency shift plots in Figure 5 for the A + 2, A + 1, and A ion peaks of the isotopic

Table 1. Frequencies and abundances recovered by FDM from the first (a) 1M, (b) 0.5 M, (c) 0.25M, (d) 0.1M, (e) 0.01M, and (f) 1000 data points of the transient signal in Figure 1b. Errors correspond to the difference between the calculated and FDM recovered frequencies.

Frequency	Intensity %	Err (ppm)
	(a)	
158906.79730	100	0.00E+00
158789.32990	5.99999792	4.41E−07
158788.50580	69.9999968	0.00E+00
158671.80090	4.00000051	−8.82E−07
158671.21309	4.00014895	4.37E−05
158670.86039	2.99979559	5.20E−05
158670.50770	25.0000252	−1.58E−06
158553.91744	2.66580469	3.74E−04
158553.33059	1.5001432	4.37E−05
158552.97840	1.99991672	1.26E−05
158552.62630	5.99995247	6.94E−07
Standard deviation		1.10E−04
	(b)	
158906.79730	99.99999	0.00E+00
158789.32990	6.000238	1.89E−06
158788.50580	70.00086	6.31E−08
158671.80090	3.999848	−1.44E−05
158671.21294	4.005262	1.04E−03
158670.85986	2.997183	3.43E−03
158670.50769	24.99762	6.57E−05
158553.91750	3.000049	2.60E−05
158553.33052	1.500441	5.31E−04
158552.97842	1.999132	−1.54E−04
158552.62630	5.992714	−2.87E−05
Standard deviation		1.05E−03
	(c)	
158906.79730	99.99997	0.00E+00
158789.32990	6.01434	4.09E−06
158788.50580	69.98557	−3.78E−07
158671.80087	4.00325	1.81E−04
158671.21081	4.04751	1.44E−02
158670.85443	2.98175	3.76E−02
158670.50759	24.97024	7.04E−04
158553.91819	2.98400	−4.37E−03
158553.33971	1.43732	−5.74E−02
158552.98745	2.05093	−5.71E−02
158552.62775	6.08859	−9.17E−03
Standard deviation		2.79E−02
	(d)	
158906.79730	100.00000	0.00E+00
158789.32990	6.00000	−1.89E−07
158788.50580	70.00000	0.00E+00
158671.77770	4.48080	1.46E−01
158671.21310	NA	0.00E+00
158670.86040	NA	0.00E+00
158670.50952	25.47574	−1.15E−02
158553.91067	3.12141	4.31E−02
158553.17399	1.24473	9.88E−01
158552.97840	NA	0.00E+00
158552.63673	6.50813	−6.58E−02
Standard deviation		2.99E−01
	(e)	
158906.79730	100.00000	6.29E−07
158789.32990	NA	0.00E+00
158788.53934	74.63911	−2.11E−01
158671.80090	NA	0.00E+00
158671.21310	NA	0.00E+00
158670.86040	NA	0.00E+00
158670.75691	36.23842	−1.57E+00
158553.86888	3.75961	3.07E−01
158553.16842	2.87426	1.02E+00
158552.97840	NA	0.00E+00
158552.74257	8.94472	−7.33E−01
Standard deviation		6.37E−01
	(f)	
158906.79719	99.99497	7.12E−04
158789.32990	NA	0.00E+00
158788.56981	75.14601	−4.03E−01
158671.80090	NA	0.00E+00
158671.21310	NA	0.00E+00
158670.86040	NA	0.00E+00
158670.75387	36.16970	−1.55E+00
158553.91750	NA	0.00E+00
158553.33060	NA	0.00E+00
158552.97840	NA	0.00E+00
158553.07004	12.50209	−2.80E+00
Standard deviation		9.14E−01

NA indicates that FDM could not resolve the frequencies within allowed error (10 ppm).

distribution respectively. While there are some FDM spurious glitches in the frequency shift plots, the isotopic peaks are clearly modulated at several different, but superimposed, frequencies. For example, all three spectra show a negative frequency dip at ~ 0.13 s and another at ~0.28 s. Additionally, there appears to be a more rapid modulation every ~0.02 s. However, these frequency shift plots are rather chaotic.

Since the monoisotopic peak at 158,760 Hz has no fine structure and satisfies the eq 9 on very short transients (1000 data points), a detailed frequency chasing experiment was expected to show a simpler and cleaner structure. Thus, a frequency chasing experiment was performed on this peak using 1 ms (1000 data points) stepping 1 μs (1 data point) into the transient for the first 0.13 s of the transient. The isotopic beat pattern is faithfully reproduced in both abundance (Figure 6b) and frequency shifts (Figure 6c). These frequency shifts occur every 0.01 s (122.07 Hz) which corresponds well with the $\Delta\omega$ between the first two isotopic peaks. Thus, these frequency shifts are clearly due to the "beating" frequency of the isotopes. Interestingly, the magnitude of this frequency shift is approximately ±75 Hz, which corresponds to ±400 ppm at ~158 kHz. However, even though the ions are shifting in frequency by ±400 ppm during the transient, the FFT is still able to achieve 1 to 2 ppm mass accuracy on this spectrum. Thus, the FFT effectively averages out these cyclic frequency shifts to achieve its results.

The level of accuracy and detail produced by these frequency shift chasing experiments depends directly on the transient signal lengths. For instance, the frequency chasing experiment in Figure 5 does not show as much modulation as Figure 6 in spite of being carried

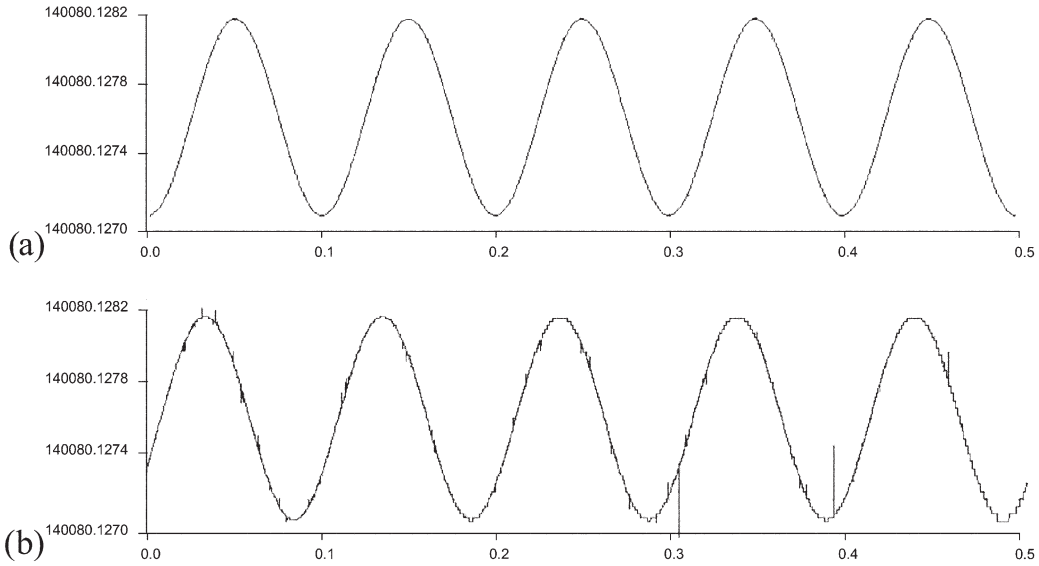

Figure 3. (**a**) a theoretical signal of 140080.1276 Hz, 0.5 S long modulated over 0.0005 Hz with frequency 10Hz, sampled at 1 MHz. (**b**) FDM output for the chasing experiment at signal to noise ratio of 2. The experiment was conducted on 500 data point transient domains stepping 200 data points into transient.

out on the same experimental dataset, due to the averaging effect. When 20 ms or, equivalently, 20,000 data points were used, the transient signal length was extended over more than one "beat" (Figure 6a) causing the averaging out of the intra "beat" frequency modulations. On the other hand, by shortening of the signal in the frequency chasing experiments, depending on the choice of a peak, reliability of the results might suffer as was discussed above.

In terms of computational performance, although FDM has the same time complexity as the FFT, it is much slower due to the computational cost of construction of the U matrices. Moreover, frequency chasing experiments scale to $(NlogN)^2$ time complexity, making these studies quite expensive. On average, a typical frequency chasing experiment, depending on the length of the transient and other parameters, takes 10 to 20 min on a Pentium IV 3.6 GHz system with 1 GB RAM running Windows XP. However, the fact that FDM is highly parallelizable makes it easy to implement it on parallel computer architecture, which will tremendously improve FDM performance and speed for frequency chasing experiments.

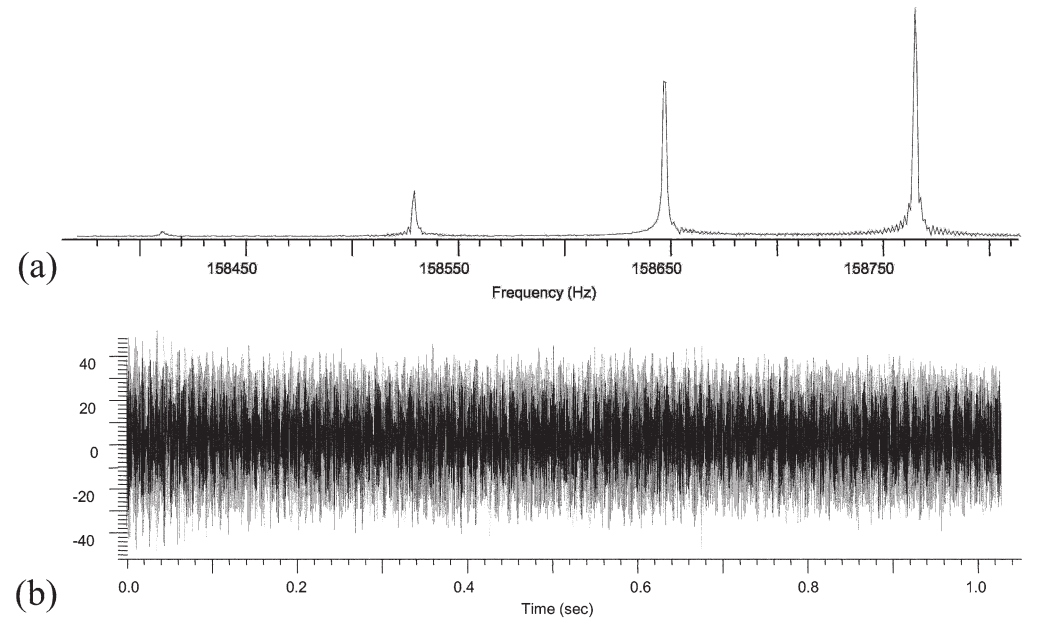

Figure 4. (**a**) frequency spectrum and (**b**) transient signal of a Substance P spectrum used for "real world" frequency chasing calculations.

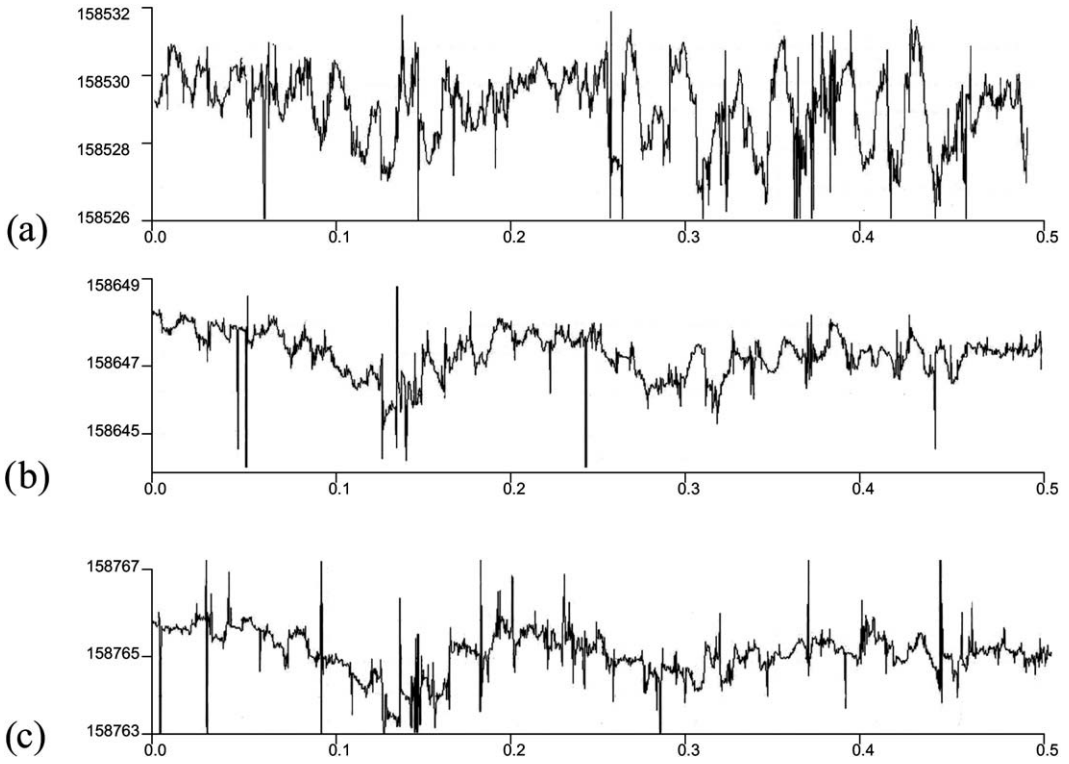

Figure 5. Frequency shift plots (20 ms, 0.2 μs shifts) of the first 0.5 s of the Substance-P spectrum (Figure 4) of the (**a**) 158530 Hz, (**b**) 158647 Hz, and (**c**) 158765 Hz peaks.

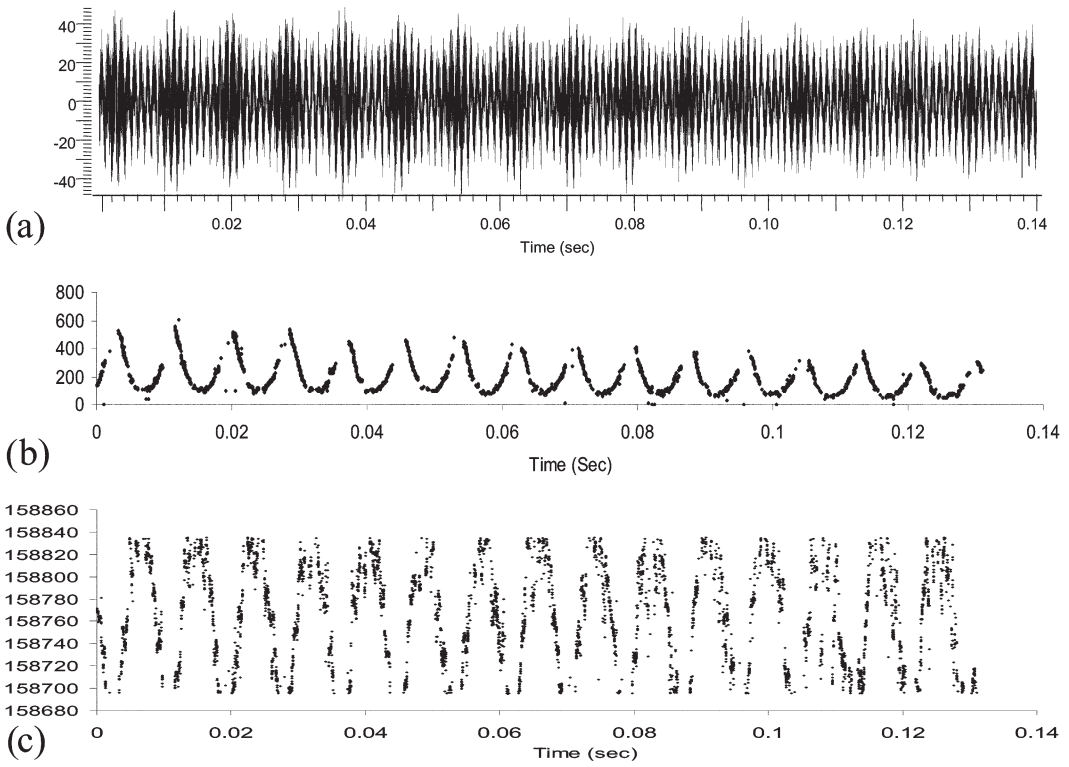

Figure 6. The frequency chasing experiment conducted on (**a**) the first 0.13 s of the Substance-P spectrum (Figure 4), chasing 158647 Hz peak using a 1K data point (1 millisecond) transient domain stepping 1 data point (1 microsecond) into the transient; (**b**) intensity versus time plot; (**c**) frequency shift plot.

Conclusions

FDM is a signal processing technique, which although slower than FFT, provides better accuracy. Computation speed and the fact that FDM requires stable resonance states (i.e., no frequency shifts) makes it a poor choice as a direct alternative to FFT in the analysis of FTMS data, which are dominated by space charge frequency shifts. In a simple Substance P spectrum, these frequency shifts are shown to reach 400 ppm. On the other hand, the improved accuracy of FDM on short transients makes it an ideal tool for frequency chasing experiments, which give a unique insight into space charge effects and provide frequency shift functions, which potentially can be used in reference deconvolution. Another area where high-resolution on short transient signals might prove useful is with LC-FTMS hybrid instruments, which attempt to operate on sub-second transients and with accurate mass measurements of short-lived radionuclides.

Acknowledgments

This work was supported in by NIH/NCRR P41-RR10888 and NIH/NHLBI NO1 HV28178. Authors acknowledge Bogdan Budnik, Cathy Costello, Jason Cournoyer, Vera B. Ivleva, Parminder Kaur, Cheng Lin, and Raman Mathur for experimental assistance and helpful discussions.

References

1. de Hoog, C. L.; Mann, M. Proteomics. *Annu. Rev. Genome Hum. Genet.* **2004,** *5,* 267–293.
2. Clauser, K. R.; Baker, P.; Burlingame, A. L. Role of accurate mass measurement (± 10 ppm) in protein identification strategies employing MS or MS/MS and database searching. *Anal. Chem.* **1999,** *71,* 2871–2882.
3. Marshall, A. G. Milestones in Fourier transform ion cyclotron resonance mass spectrometry technique development. *Int. J. Mass Spectrom.* **2000,** *200,* 331–356.
4. Comisarow, M. B.; Marshall, A. G. Fourier transform ion cyclotron resonance spectroscopy. *Chem. Phys. Lett.* **1973,** *25,* 282–283.
5. Marshall, A. G.; Hendrickson, C. L.; Shi, S. D. Scaling MS plateaus with high-resolution FT-ICRMS. *Anal. Chem.* **2002,** *74,* 252A–259A.
6. Lorenz, S. A.; Moy, M. A.; Dolan, A. R.; Wood, T. D. Electrospray ionization Fourier transform mass spectrometry quantification of enkephalin using an internal standard. *Rapid Commun. Mass Spectrom.* **1999,** *13,* 2098–2102.
7. O'Connor, P. B.; Costello, C. E. Internal calibration on adjacent samples (InCAS) with Fourier transform mass spectrometry. *Anal. Chem.* **2000,** *72,* 5881–5885.
8. Flora, J. W.; Hannis, J. C.; Muddiman, D. C. High-mass accuracy of product ions produced by SORI-CID using a dual electrospray ionization source coupled with FTICR mass spectrometry. *Anal. Chem.* **2001,** *73,* 1247–1251.
9. Easterling, M. L.; Mize, T. H.; Amster, I. J. MALDI FTMS Analysis of polymers—improved performance using an open ended cylindrical analyzer cell. *Int. J. Mass Spectrom. Ion Processes* **1997,** *169,* 387–400.
10. Hannis, J. C.; Muddiman, D. C. A dual electrospray ionization source combined with hexapole accumulation to achieve high mass accuracy of biopolymers in Fourier transform ion cyclotron resonance mass spectrometry. *J. Am. Soc. Mass Spectrom.* **2000,** *11,* 876–883.
11. Spengler, B. De novo sequencing, peptide composition analysis, and composition-based sequencing: A new strategy employing accurate mass determination by Fourier transform ion cyclotron resonance mass spectrometry. *J. Am. Soc. Mass Spectrom.* **2004,** *15,* 703–714.
12. Norbeck, A. D.; Monroe, M. E.; Adkins, J. N.; Anderson, K. K.; Daly, D. S.; Smith, R. D. The utility of accurate mass and LC elution time information in the analysis of complex proteomes. *J. Am. Soc. Mass Spectrom.* **2005,** *16,* 1239–1249.
13. Wineland, D.; Dehmelt, H. Line shifts and widths of axial, cyclotron, and G-2 resonances in tailored, stored electron (ion) cloud. *Int. J. Mass Spectrom.* **1975,** *(a)*, 338–342.
14. Press, W. H.; Teukolsky, S. A.; Vetterling, W. T.; Flannery, B. P. *Numerical recipes in C*, 2nd ed., *The art of scientific computing*; Cambridge University Press: Ithaca, NY, 1992.
15. Mann, S.; Haykin, S. Adaptive "chirplet" transform: An adaptive generalization of the wavelet transform. *Opt. Eng.* **1992,** *31,* 1243–1256.
16. Savitski, M. M.; Ivonin, I. A.; Nielsen, M. L.; Zubarev, R. A.; Tsybin, Y. O.; Hakansson, P. Shifted-basis technique improves accuracy of peak position determination in Fourier transform mass spectrometry. *J. Am. Soc. Mass Spectrom.* **2004,** *15,* 457–461.
17. Guan, S.; Marshall, A. G. Linear prediction Cholesky decomposition versus Fourier transform spectral analysis for ion cyclotron resonance mass spectrometry. *Anal. Chem.* **1997,** *69,* 1156–1162.
18. Loo, J. F.; Krahling, M. D.; Farrar, T. C. Accurate ion abundance measurements in ICR/MS by linear prediction. *Rapid Commun. Mass Spectrom.* **1990,** *4,* 297–299.
19. Marple, S. L. *Digital spectral analysis: with applications*; Prentice-Hall, Inc.: Upper Saddle River, NJ, 1986.
20. R. Roya; B. G. Sumpterc; G. A. Pfefferd; S. K. Graye ; Noidc, D. W. Novel methods for spectral analysis. *Phys. Rep.* **1991, *205,*** 109–152.
21. Wall, M. R.; Neuhauser, D. Extraction, through filter-diagonalization, of general quantum Eigen values or classical normal-mode frequencies from a small number of residues or a short-time segment of a signal. 1. Theory and application to a quantum-dynamics model. *J. Chem. Phys.* **1995,** *102,* 8011–8022.
22. Hu, H.; Van, Q. N.; Mandelshtam, V. A.; Shaka, A. J. Reference deconvolution, phase correction, and line listing of NMR spectra by the 1D filter diagonalization method. *J. Magn. Reson.* **1998,** *134,* 76–87.
23. Mandelshtam, V. A. FDM: The filter diagonalization method for data processing in NMR experiments. *Prog. Nucl. Magn. Reson. Spectrosc.* **2001,** *38,* 159–196.
24. Mandelshtam, V. A. On harmonic inversion of cross-correlation functions by the filter diagonalization method. *J. Theor. Comp. Chem.* **2003,** *2,* 497–505.
25. Mandelshtam, V. A.; Taylor, H. S. A low-storage filter diagonalization method for quantum Eigen energy calculation or for spectral analysis of time signals. *J. Chem. Phys.* **1997,** *106,* 5085–5090.
26. Mandelshtam, V. A.; Taylor, H. S. Spectral analysis of time correlation function for a dissipative dynamical system using filter diagonalization: Application to calculation of unimolecular decay rates. *Phys. Rev. Lett.* **1997,** *78,* 3274–3277.
27. Mandelshtam, V. A.; Taylor, H. S. Harmonic inversion of time signals and its applications. *J. Chem. Phys.* **1998,** *109,* 4128–4128.
28. Bruce, J. E.; Anderson, G. A.; Hofstadler, S. A.; Winger, B. E.; Smith, R. D. Time-base modulation for the correction of cyclotron frequency shifts observed in long-lived transients from Fourier-transform ion-cyclotron-resonance mass spectrometry of electrosprayed biopolymers. *Rapid Commun. Mass Spectrom.* **1993,** *7,* 700–703.
29. Guan, S.; Wahl, M. C.; Marshall, A. G. Elimination of frequency drift from FTICR mass spectra by digital quadrature heterodyning: Ultrahigh mass resolving power for laser-desorbed molecules. *Anal. Chem.* **1993,** *65,* 3647–3653.
30. O'Connor P, B. Boston University Data Analysis (B.U.D.A.) 2002. http://www.bumc.bu.edu/ftms
31. Frigo, M. The design and implementation of FFTW3. *Proc. IEEE* **2005,** *93,* 216–231.
32. Anderson, E.; Bai, Z.; Bischof, C.; Blackford, S.; Demmel, J.; Dongarra, J.; Du Croz, J.; Greenbaum, A.; Hammarling, S.; McKenney, A. a. S. D. *LAPACK User's Guide*; Society for Industrial and Applied Mathematics: Philadelphia, PA, 1999.
33. Senko, M. IsoPro 3.0; http://members.aol.com/msmssoft/ISOPRO30.HTM
34. Yergey, J. A. A general approach to calculating isotopic distributions for mass spectrometry *Int. J. Mass Spectrom. Ion Processes* **1983,** *52,* 337–349.
35. Pittman, J. L., Thomson, B. A., and O'Connor, P. B. A novel hybrid instrument using a commercial electrospray ionization source with a high-performance FTMS for proteomics applications. *Proceedings of the 52nd ASMS Conference*; Nashville, TN, 2004.
36. Jebanathirajah, J. A.; Pittman, J. L.; Thomson, B. A.; Budnik, B. A.; Kaur, P.; Rape, M.; Kirschner, M.; Costello, C. E.; O'Connor, P. B. Characterization of a new QqQ-FTICR mass spectrometer for post-translational modification analysis and top-down tandem mass spectrometry of whole proteins. *J. Am. Soc. Mass Spectrom.* **2005,** *16,* 1985–1999.
37. O'Connor, P. B.; Pittman, J. L.; Thomson, B. A.; Budnik, B. A.; Cournoyer, J. C.; Jebanathirajah, J.; Lin, C.; Moyer, S. A New hybrid electrospray Fourier transform mass spectrometer: Design and performance characteristics. *Rapid. Commun. Mass Spectrom.* **2006,** *20,* 259–266.
38. Stolzenberg, H.; Becker, S.; Bollen, G.; Kern, F.; Kluge, H.; Otto, T.; Savard, G.; Schweikhard, L.; Audi, G.; Moore, R. B. Accurate mass determination of short-lived isotopes by a tandem Penning-trap mass spectrometer. *Phys. Rev. Lett.* **1990,** *65,* 3104–3107.